STUDY OF THERMAL DIFFUSIVITY AND MICROSTRUCTURE IN API5L-X52 CARBON STEEL[1]

G. Peña-Rodríguez[2,3,4,5], Oscar Flores-Macias[3], C. Angeles-Chavez[3], R. A. Muñoz-Hernández[2] and A. Calderón[2,5]

[1] Paper presented at the Fifteenth Symposium on Thermophysical Properties, June 22-27, 2003, Boulder, Colorado, U.S.A.
[2] Centro de Investigación en Ciencia Aplicada y Tecnología Avanzada del IPN, Legaria 694 Colonia Irrigación, 11500 México D. F.
[3] Instituto Mexicano del Petróleo, Eje Central L. Cárdenas 152, Colonia San Bartolo Atepehuacan, 07730 México D. F.
[4] Departamento de Física, Universidad Francisco de Paula Santander A. A. 1055, Cúcuta, Colombia.
[5] To whom correspondence should be addressed, E-mail: ggabrielp@yahoo.com or calder620831@aol.com

ABSTRACT

By means of the photoacoustic technique in a heat transmission configuration we realize the thermal diffusivity (α) determination in API5L-X52 steel for manufacturing pipelines. Besides this, we present a study of the microstructure of this low carbon steel by mean of scanning electronic microscopy (SEM) and X ray diffraction (XRD). We report our α results and we did a comparison with the literature reported values for the steel with similar composition to the API5L-X52 steel. Nowadays do not exist reported values of thermal diffusivity for this low carbon steel. Our obtained value for the thermal diffusivity in API5L-X52 steel is in the same magnitude order of reported values of other types of low carbon steel, 50% less than the α value of pure iron, 30% less than the α value of 1018 steel and 12% less than the α value of 1020 steel. The comparison between XRD and SEM results show that the main phase in this low carbon steel is the ferrous one.

KEY WORDS: API5L-X52 carbon steel, microsctructure, thermal diffusivity.

1. INTRODUCTION

The knowledge of microstructure, physical and chemical properties of materials and the relation among each other, are of interest in the selection of materials that will be used in the design and manufacturing of pipelines with certain specifications that they have to fulfill for installation, operation and maintenance of the fluid transportation. In the last years, the study of the relation between mechanical and thermal properties has interested to the steel and metal industries, as a proof of this we can see the studies about the relation between hardness and thermal diffusivity (α) of steel [1, 2] .

The thermal wave propagation in solid materials is influenced by microstructure characteristics, size and grain boundary, impurities and imperfections, all of them contribute to the energy dispersion of the carriers like phonons and electrons inside the material, giving a decreasing in the heat flow through of material [3, 4]. The decreasing in the grain size in ferrous steel of low concentration of carbon, allows the increasing in the mechanical resistance of material and then a better resistance to fractures [5, 6].

There is a big number of works on stress corrosion cracking (SCC) and microbiologically influenced corrosion (MIC) in metals and mainly in steel carbon used in petroleum and its refined products, where the knowledge of the metal microstructure is important for to study and depending on certain conditions the corrosion in metals decrease while the temperature increases [7 -8].

In Mexico, there are operating more than fifty thousand kilometers of terrestrial pipelines and about of two thousand kilometers in submarine zones, they carry petroleum and its derivative products [9]. The realization of studies that help to increase the security of transportation of oil products is very important.

Because of we mentioned before and we do not find reported values of thermal diffusivity for 5L specification and X52 grade in the American Petroleum Institute (API) [10,11], in this work we determined the thermal diffusivity values by means the photoacoustical technique in a heat transmission configuration at room temperature, this technique has been widely used in the thermal characterization of solids [12-14], and we did a microstructural analysis of this material using scanning electronic microscopy (SEM) and x ray difracction (XRD).

2. MEASUREMENTS

2.1. Specimens

Using a low speed disc cutter (South Bay Technology SBT-650) and diamond edge discs (Buehler 11-4244), five cuts of few hundreds of micrometers of thickness and one cm^2 of surface were made to the wall of 6.35 mm of thickness of one pipeline section of 127 mm

of internal ratio of API grade X52 carbon steel and chemical composition in weight percentage of: 0.092 % C, 1.03 % Mn, 0.014 % P, 0.005 % S, < 0.005 % Nb, <0.001 % V y < 0.002 % Ti. The samples thickness shown in Table I were accomplished using a low speed polishing machine (SBT- 910) and abrasive paper (Buehler 30-5118-240). The thickness of the samples were measured using a digital micrometer (Mitutoyo 543-252). In order to avoid the oxidation of clean samples surfaces, these were put in glass container with silica gel. For metalographic processes we use one micrometer diamond paste (Buehler Metadi II) and polishing cloths (Buehlr 40-7218), the structure of material were revealed by chemical attack using nital 0.2% solution for ten seconds.

2.2. Procedure

Since the presentation of the open photoacoustic cell (OPC) for thermal characterisation of solids [15], this method has been widely used in the measurement of the thermal properties of a large variety of materials [12]. The OPC method consists of mounting the sample under study directly onto a commercial electret microphone [16], using the front chamber of the microphone itself as the usual gas chamber of conventional photoacoustics. Its advantage over conventional photoacoustic cells is the use of a minimal gas chamber with no further transducer medium needed, no cell machining required, and low cost.

From the one-dimensional thermal diffusion model one gets that the amplitude of the OPC signal for optically opaque samples is [13]

$$A = \frac{C}{f\sqrt{\cosh(2l_s\sqrt{\pi f/\alpha}) - \cos(2l_s\sqrt{\pi f/\alpha})}} \qquad (1)$$

In this expression f is the modulation frequency, α is the thermal diffusivity of the sample, L its thickness and C a parameter constant that depends of: the pressure, thermal properties of the air inside the acoustic chamber, light intensity and cell geometry of the photoacoustic cell. The thermal diffusivity sample can be obtained by means of fitting the expression (1) to of signal amplitude data [13,14].

The study of microstructure of the samples was realized using an X ray difractometer Siemems D-5000 and scanning electron microscope PHILIPS ESEM-XL30.

3. RESULTS AND DISCUSSION

In Table I, we present the experimental results of thermal diffusivity of five API5L-X52 low carbon steel samples. We can see that the α obtained values has not a significant variation between one and other sample and we get a average value of α = 0.116 cm^2/s with 5% error approximately. Figure 1 show the PA signal amplitude versus modulation frequency, the curve indicate the best fitting of the Eq. (1) to experimental data.

From the α reported values for other types of low carbon steel, table II, we can see that the α value increase with the concentration of carbon and Mn in the material. Thermal

diffusivity of API5L-X52 steel result 50% less than α value of pure iron, 30% less than α value of 1018 steel and 12% less than α value of 1020 steel value [17, 18].

In Figure 2, we present the X ray diffraction patterns of the API5L-X52 steel samples. The peaks represent the crystalline planes (110), (200), (211) and (220), they correspond with the body centered cubic (bcc) structure of the α-Fe phase, with a lattice parameter value of 2.8664 angstroms. In determining this we used the JCPDS-ICDD 6-0696 card and we do not appreciate differences between the constitutive phases of samples.

In Figure 3, we present the API5L-X52 steel microstructure, with a 500X amplification. It was obtained using SEM, in this Figure we can see that the main phase is the α-Fe (b), which corresponds with the XRD results, we can see small lamellar areas of pearlite phase (a) and solid inclusions (c). We show in Figure 4 a 2000X amplification of these inclusions (c) with a 79.4 particles per mm^2. In Table III, we present a quantitative analysis using EDS-SEM of the inclusions, its corresponding spectrum is presented in Figure 5.

In figure 6 we show the grain size distribution of the α-Fe phase and grain size distribution for the inclusion particles is showed in Figure 7. Using the ASTM E112-96 we determined the α-Fe phase and the inclusions grain size values, 6.084 μm and 3.027 μm respectively.

ACKNOWLEDGMENT

The autors would like to thank to the following persons: Ignacio Loza Martínez of CICATA-IPN who prepared the samples, Ph. D Cheng Dong the Institute of Physics of the Chinese Academy of Science for giving us the permission of the use of the software Powder X. This work was partially supported by the project No. D.00049 of the Instituto Mexicano del Petróleo, by CGPI-IPN and the PIFI-IPN program.

REFERENCES

1. D. Fournier, JP Roger, A. Bellouati, C. Boué, H. Stam and F. Lakestani. *Analytical Science* **17**: s158, (2001).
2. H. G. Walther, D. Fournier, J.C. Krapez, M. LuuKKala, B. Schmitz, C. Sibilia, H. Stamm and J. Thoen. *Analytical Science* **17**: s165 (2001).
3. Ton Thi Ngoc Lan, Heinz-Gunter Walther and Do Tran So, *High Temperature – High Pressures* **29**: 165 (1997).
4. Yoshihiro Terada, Kenji Ohkubo, Tetsuo Mohri and Tomoo Suzuki. *Metallurgical and Materials Transactions* **32 A**: 2135 (2001).
5. R. Priestner and A.K. Ibraheem. *Materials Science and Technology* **16**:1267 (2000).
6. P.J. Hurley, G. L. Kely and P. D. Hodgson. *Materials Science and Technology* **16**:1273 (2000).
7. Juan J. González and Alexander Bentolila, *Corrosion Technology* **83**: 5 (2000)
8. R. Nishimura, I. Katim and Y. Maeda, *Corrosion* **57**: 853 (2001).
9. *La investigación en el Instituto Mexicano del Petróleo*, Vol. 107, (IMP, México, 2000).
10. E-mail communication with **Mike Spanhel.** Coordinator, Upstream Standards,

American Petroleum Institute, 1220 L Street, NW,Washington, DC 20005-4070, Tel 202-682-8292, E-mail spanhel@api.org
11. E-mail communication with **Marie T Brisman.** NACE International. Member Service Department. E-mail: marie@mail.nace.org
12. A. Calderón, J.J. Alvarado, Yu. G. Gurevich, A. Cruz Orea, I. Delgadillo H. Vargas and L.C.M. Miranda. *Physical Review Letters* **79**:5022 (1997).
13. A. Calderón, R.A. Muñoz Hernández, S.A. Tomás, A. Cruz Orea and F. Sánchez Sinencio. *J. Appl. Phys* **84**: 6327 (1998).
14. G. Peña Rodríguez, A. Calderón Arenas, R.A. Muñoz Hernández, S. Stolik, A: Cruz Orea and F. Sánchez Sinencio, *Analytical Science* **17**:s357 (2001).
15 L. F. Perondi and L. C. M. Miranda, *J. Appl. Phys.* **62**:2955 (1987)
16 G. M. Sessler, J. E. West, *J. Acoust. Soc. Am.* **53**: 1589 (1973).
17. D.P. Almond and P.M. Patel, *Photothermal science and techniques*, (Chapman & Hall, London, 1996), pp. 16-17.
18. Y. S. Touloukian, *Thermophysical Properties of Matter*, Vol. 10 (IFI/Plenum, New York, 1973)

Table I. Thermal diffusivity for API5L-X52 carbon steel samples.

SAMPLES	l_s **(μm)**	α **x** 10^{-3} **(cm^2/s)**
A1	167 ± 3	118 ± 5
A2	170 ± 3	116 ± 5
A3	175 ± 6	116 ± 6
A4	176 ± 3	116 ± 5
A5	170 ± 5	115 ± 6

Table II. Thermal diffusivity values at room temperature reported for some types of low carbon steel [17, 18].

SAMPLES	C (% Wt)	Mn (% Wt)	α x 10^{-3} (cm^2/s)
Fe Pure	-	-	227
SAE 1010	0.1	0.42	191
Steel 1018	0.18	~ 0.50	165
Steel 1020	0.20	~ 0.60	130

Table III. Results of quantitative elementary analysis using EDS-SEM for the inclusion particle observed in figure 4.

Element	O	Mg	Al	S	S	Ca	Mn	Fe
Wt %	14.47	2.60	33.07	6.41	3.76	2.27	7.95	30.23

Figure Captions

Fig. 1. PA signal amplitude versus frequency, The curve indicate the best fitting of the Eq. (1) to experimental data.

Fig. 2. XRD patterns for API5L-X52 carbon steel samples.

Fig. 3. SEM image showing the microstructure of the API5L-X52 carbon steel by 500X. a) pearlite, b) α-Fe phase, and c) some inclusion in the structure. (etched in 0.2% nital by ten seconds).

Fig. 4. SEM image showing the microstructure of the API5L-X52 by 2000X, the micrograph shows a typical solid inclusion particle c).

Fig. 5. Espectra of quantitative elementary analysis using EDS-SEM for the inclusion particle observed in figure 4 and presented in table III.

Fig. 6. Grain size distribution for the ferrite phase.

Fig. 7. Grain size distribution for the inclusion particles.

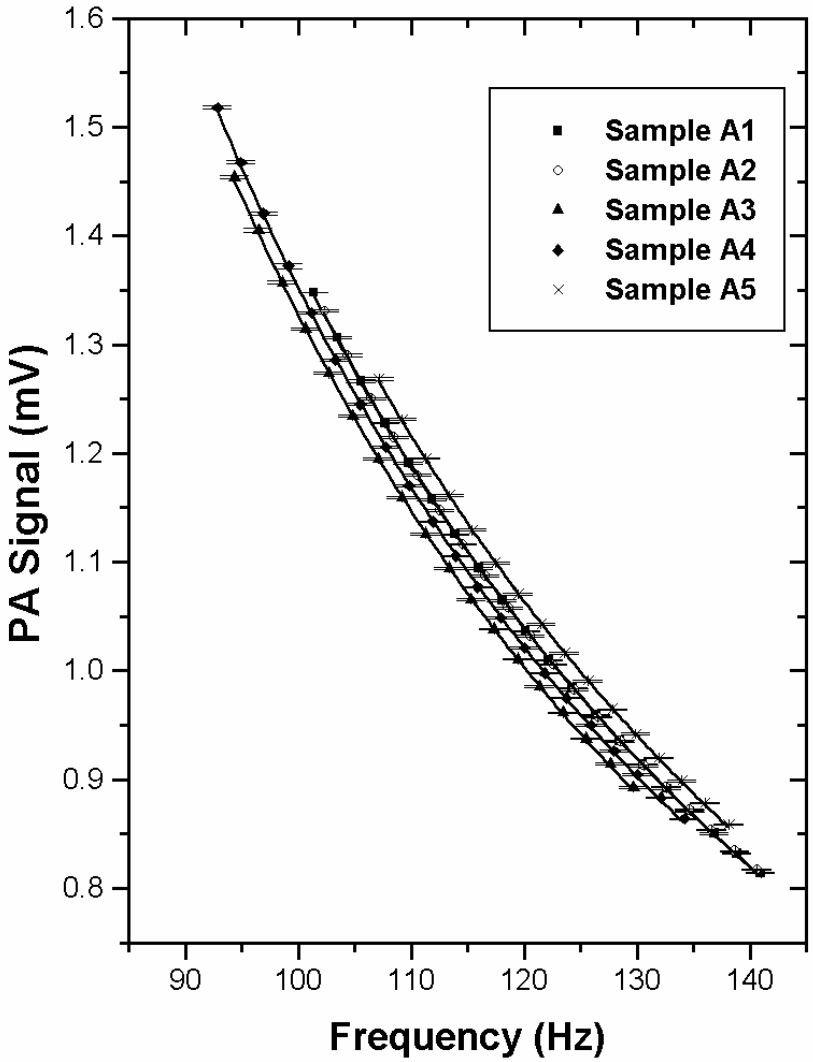
PA Signal (mV)
Frequency (Hz)
Sample A1
Sample A2
Sample A3
Sample A4
Sample A5
1.6
1.5
1.4
1.3
1.2
1.1
1.0
0.9
0.8
90
100
110
120
130
140

Fig. 1

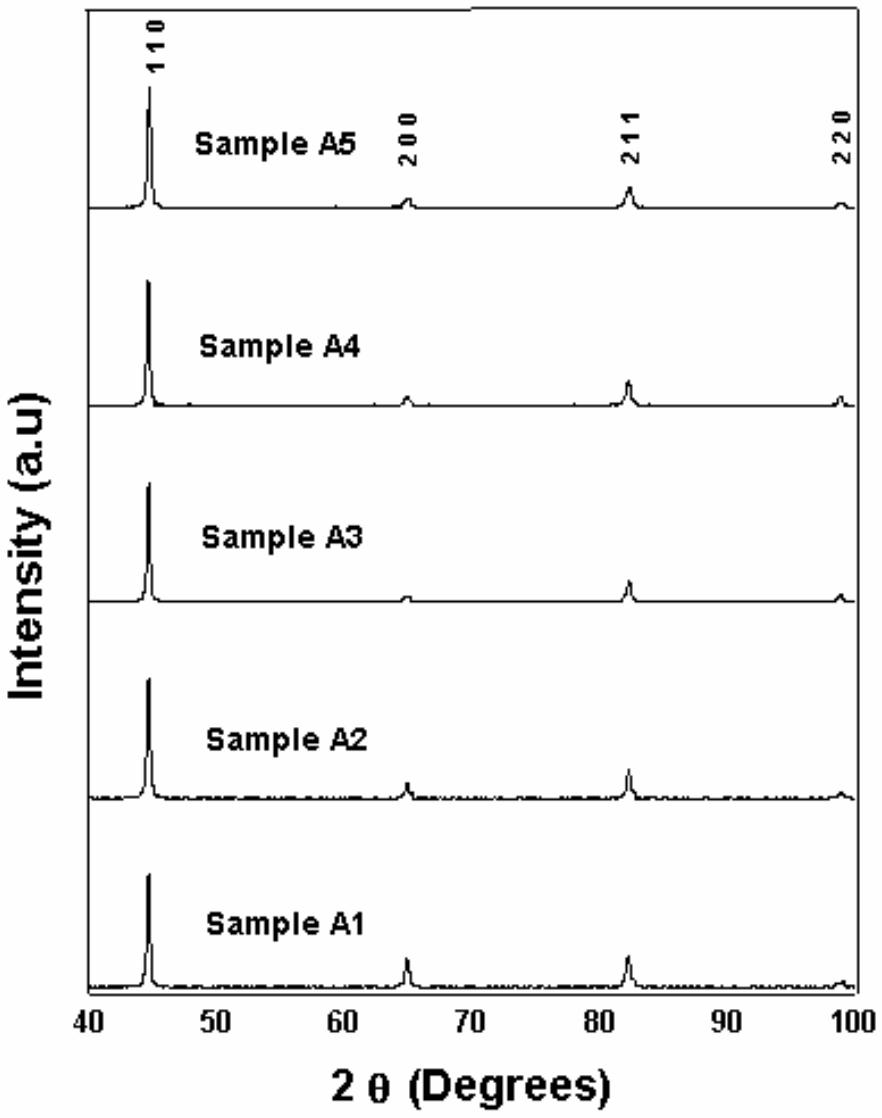
1 1 0
2 0 0
2 1 1
2 2 0
Sample A5
Sample A4
Sample A3
Sample A2
Sample A1
Intensity (a.u)
40
50
60
70
80
90
100
2 θ (Degrees)

Fig. 2

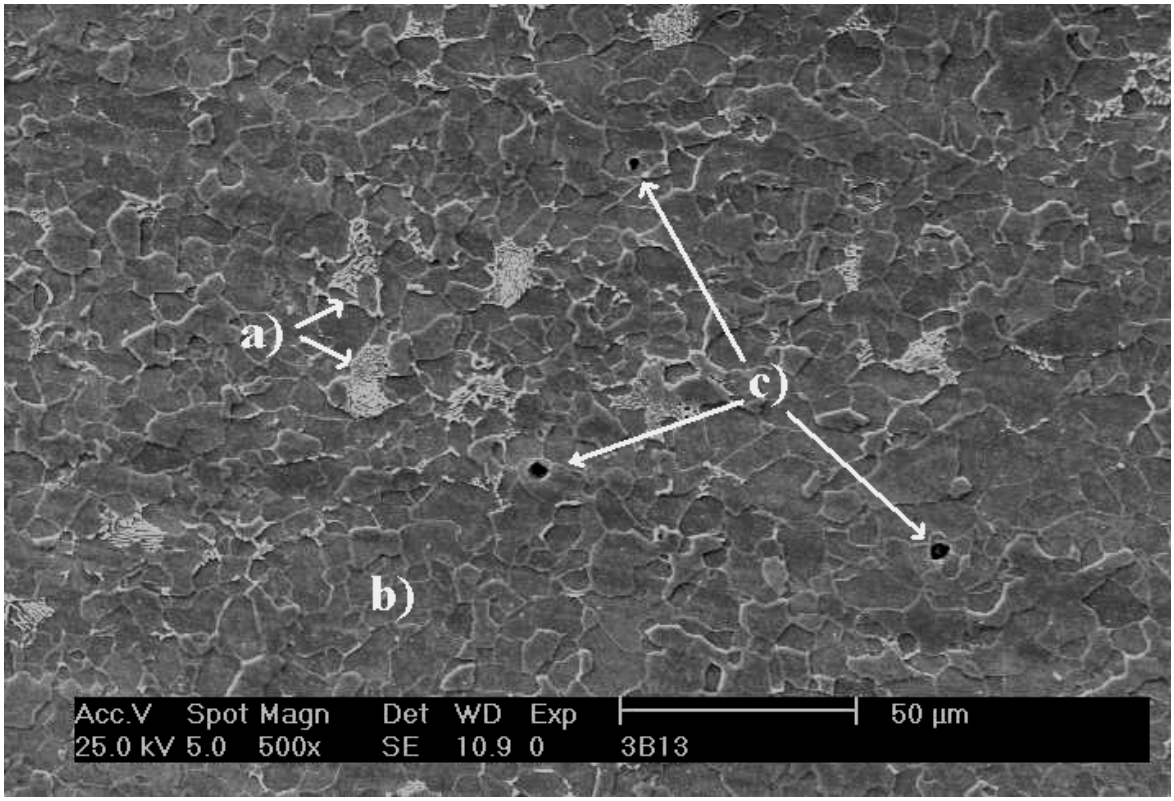

Fig. 3

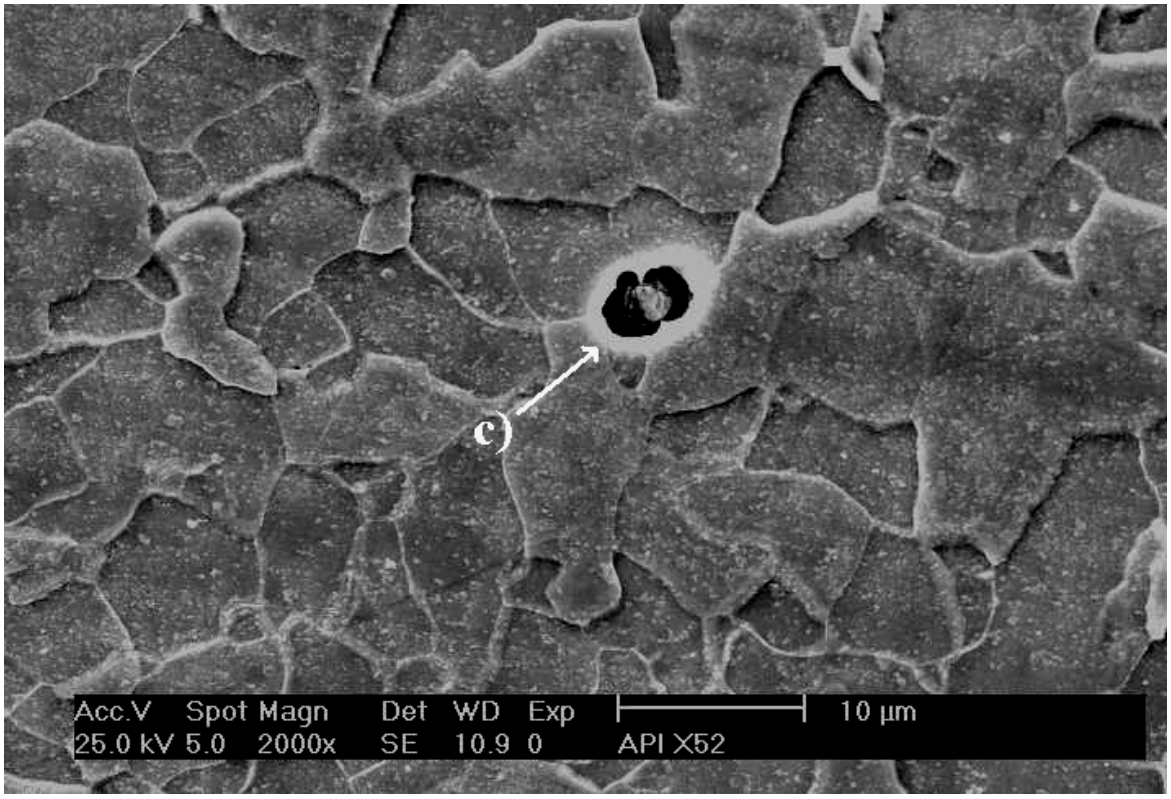

Fig. 4

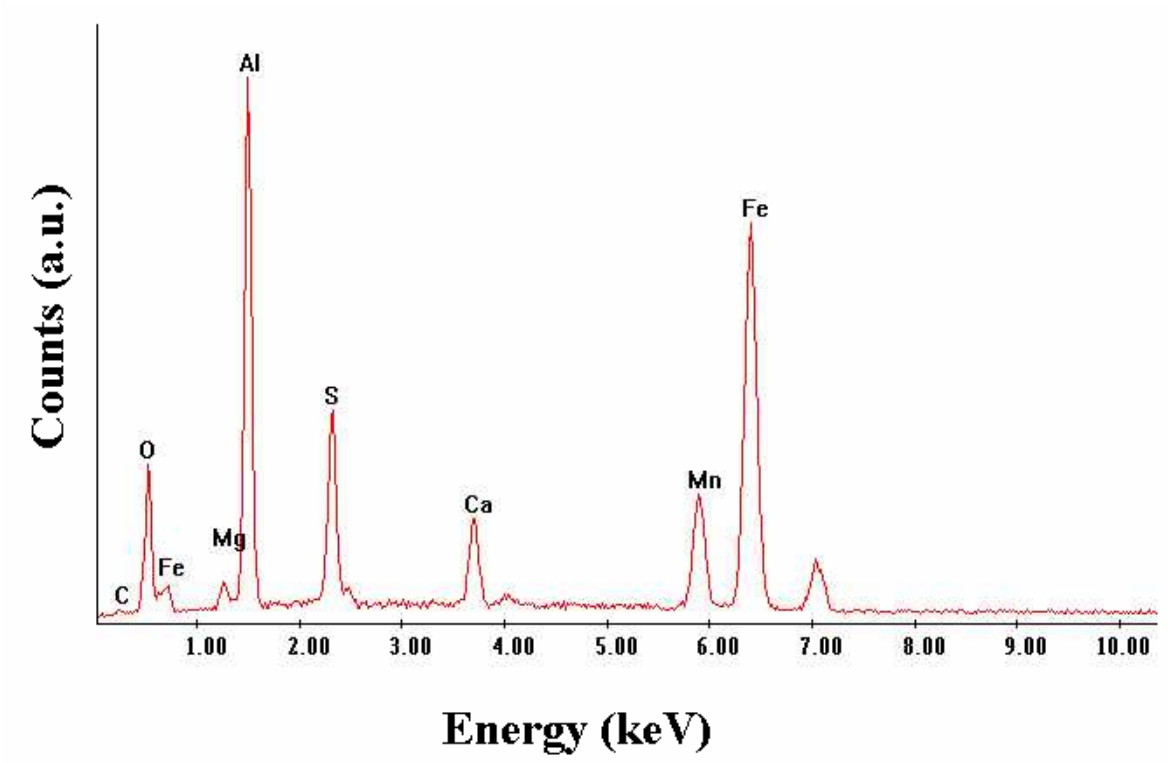
Counts (a.u.)
Al
Fe
S
O
Mn
Ca
Mg
Fe
C
1.00
2.00
3.00
4.00
5.00
6.00
7.00
8.00
9.00
10.00
Energy (keV)

Fig. 5

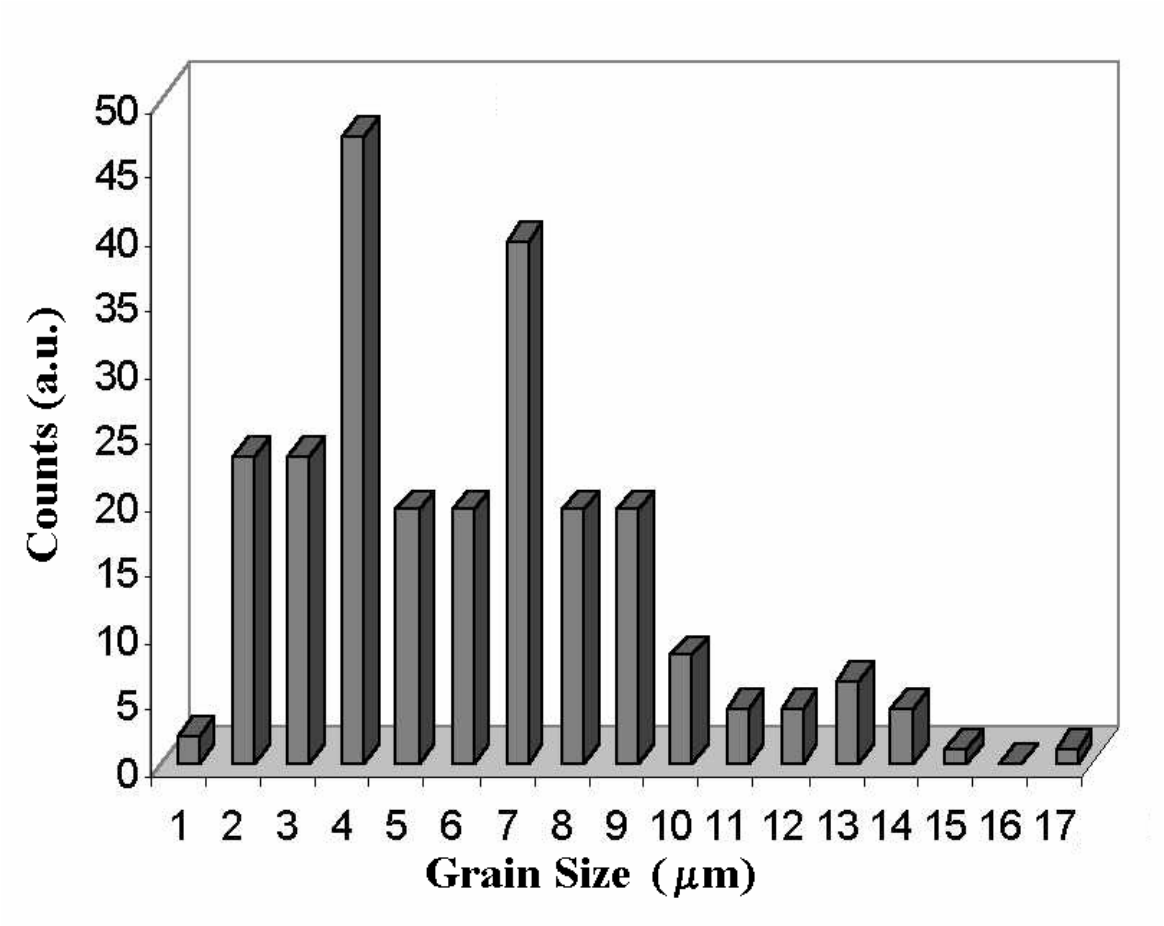
Counts (a.u.)
0
5
10
15
20
25
30
35
40
45
50
1 2 3 4 5 6 7 8 9 10 11 12 13 14 15 16 17
Grain Size (μm)

Fig. 6

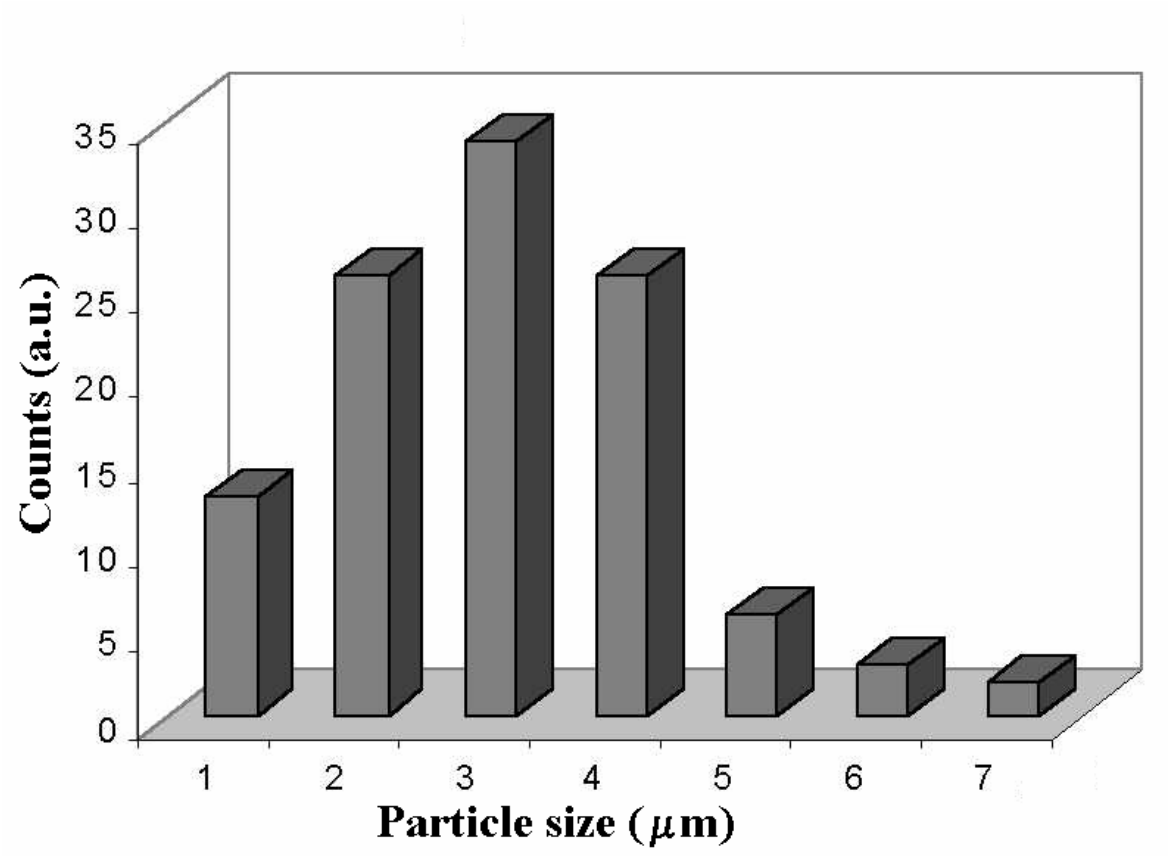

Fig. 7